Human Genetics
https://doi.org/10.1007/s00439-025-02761-x

ORIGINAL INVESTIGATION

Genomic and molecular evidence that the LncRNA *DSP-AS1* modulates desmoplakin expression

Luisa Foco[1] · Marzia De Bortoli[1] · Fabiola Del Greco M[1] · Laura S. Frommelt[1,2,3] · Chiara Volani[1,4] · Diana A. Riekschnitz[1] · Benedetta M. Motta[1] · Christian Fuchsberger[1] · Thomas Delerue[5] · Uwe Völker[6,7] · Tianxiao Huan[8,9] · Martin Gögele[1] · Juliane Winkelmann[10] · Marcus Dörr[7,11] · Daniel Levy[8,9] · Melanie Waldenberger[5,12] · Alexander Teumer[7,13] · Peter P. Pramstaller[1] · Alessandra Rossini[1] · Cristian Pattaro[1]

Received: 28 April 2025 / Accepted: 5 July 2025

Abstract

Cardiac desmosomes are specialized cell junctions responsible for cardiomyocytes mechanical coupling. Mutation in desmosomal genes cause autosomal dominant and recessive familial arrhythmogenic cardiomyopathy. Motivated by evidence that Mendelian diseases share genetic architecture with common complex traits, we assessed whether common variants in any desmosomal gene were associated with cardiac conduction traits in the general population. We analysed data of N=4342 Cooperative Health Research in South Tyrol (CHRIS) study participants. We tested associations between genotype imputed variants covering the five desmosomal genes Desmoplakin (*DSP)*, junction plakoglobin *(JUP)*, plakophilin 2 *(PKP2)*, desmoglein 2 *(DSG2)*, and desmocollin 2 *(DSC2)*, and P-wave, PR, QRS, and QT electrocardiographic intervals, using linear mixed models. Functional annotation and interrogation of publicly available genome-wide association study resources implicated potential connection with antisense long non-coding RNAs (lncRNAs), DNA methylation sites, and complex traits. Causality was tested via two-sample Mendelian randomization (MR) analysis and validated with functional in vitro follow-up in human induced pluripotent stem cell derived cardiomyocytes (hiPSC-CMs). *DSP* variant rs2744389 was associated with QRS ($P=3.5\times10^{-6}$), with replication in the Microisolates in South Tyrol (MICROS) study (n=636; P=0.010). Observing that rs2744389 was associated with *DSP-AS1* antisense lncRNA but not with *DSP* expression in multiple Genotype-Tissue Expression (GTEx) v8 tissues, we conducted two-sample Mendelian randomization analyses that identified causal effects of *DSP-AS1* on *DSP* expression ($P=6.33\times10^{-5}$; colocalization posterior probability=0.91) and QRS (P=0.015). In hiPSC-CMs, *DSP-AS1* expression downregulation through a specific GapmerR matching sequence led to significant *DSP* upregulation at both mRNA and protein levels. The evidence that *DSP-AS1* has a regulatory role on *DSP* opens the venue for further investigations on *DSP-AS1*'s therapeutic potential for conditions caused by reduced desmoplakin production.

Introduction

Cardiac desmosomes are specialized cell junctions responsible for cardiomyocytes mechanical coupling. The cardiac desmosome includes the proteins Desmoplakin (*DSP*), Plakophilin-2 (*PKP2*), Desmoglein-2 (*DSG2*), Desmocollin-2 (*DSC2*), and Junction Plakoglobin (*JUP*).

Dysfunctional desmosomes can lead to cardiomyocyte detachment during contraction, altering the mechano-electrical coupling between cells and triggering arrhythmias (Sen-Chowdhry et al. 2005), but also to aberrant activation of signalling pathways such as Wnt/β-catenin signalling (Garcia-Gras et al. 2006), the Hippo (Chen et al. 2014) and TGFβ (Schinner et al. 2022) pathways, which have previously been described to play a pivotal role in

Alessandra Rossini and Cristian Pattaro have conducted joint supervision.

Luisa Foco and Marzia De Bortoli have contributed equally to the manuscript.

Extended author information available on the last page of the article

Published online: 30 July 2025

Arrhythmogenic Cardiomyopathy (ACM) pathology, regulating both adipogenesis and fibrogenesis. In fact, pathogenic variants in desmosomal genes have been frequently involved in ACM, a familial disease, with an autosomal dominant pattern of inheritance with reduced penetrance (Sharma et al. 2022). Homozygous desmosomal gene mutations have also been described to cause recessive forms of ACM (Austin et al. 2019). ACM is a primary structural cardiomyopathy characterized clinically by life-threatening arrhythmias, increasing the risk of sudden cardiac death. In symptomatic patients, specific electrocardiogram (ECG) abnormalities such as epsilon waves are observed together with palpitations, arrhythmic presyncope/syncope and ventricular tachyarrhythmias (Elliott et al. 2019; Towbin et al. 2019). Despite about 26 genes having been implicated in ACM, the ClinGen Cardiovascular Clinical Domain Working Group has indicated that only the five desmosomal genes *DSP*, *PKP2*, *DSG2*, *DSC2*, and *JUP*, and transmembrane protein 43 *(TMEM43)* are definitively linked to ACM (James et al. 2021).

According to polygenic theory, Mendelian traits can be regarded as extreme manifestations of common complex traits, hence sharing genetic architecture (Blair et al. 2013). This implies the existence of a spectrum of differential severity observed even within Mendelian phenotypes, indicating that different mutations in the same gene can have a different impact. By extension, a relevant question to ask is whether mutations in ACM genes are associated with altered ECG signatures in individuals not selected for any cardiac disease. For instance, ACM cases were identified in the Finnish general population by typing 6 rare *DSP*, *DSG2*, *DSC2* and *PKP2* variants tested against the PR, QT, QRS, and RR intervals in 6334 individuals, resulting in significant associations with PR at *DSP* and *PKP2* (Lahtinen et al. 2011).

Expanding this idea, we designed an investigation that assessed whether any common genetic variant located within any of the 5 definitive ACM desmosomal genes (*DSP*, *PKP2*, *DSG2*, *DSC2*, and *JUP*) were associated with cardiac conduction traits in a general population sample. Because ACM patients show conduction abnormalities in depolarization and repolarization, we selected as study outcomes the length of the P-wave, and the PR, QRS, and QT intervals. Building on significant results, we designed Mendelian randomization (MR) experiments to assess if the associated genes had a causal effect on the respective ECG traits. MR was further implemented to assess causal connections between the molecular entities involved by the variant-ECG association, namely mRNA levels of *DSP* and of *DSP* antisense 1 (*DSP-AS1*) long-non-coding RNA (lncRNA), and the cg02643433 methylation. Evidence of a causal effect of the *DSP-AS1* lncRNA on *DSP*, eventually led us to functionally demonstrate the role of *DSP-AS1* on *DSP* gene expression in human induced pluripotent stem cell derived cardiomyocytes (hiPSC-CMs).

Methods

Discovery and replication studies

Considered in these analyses were 4342 participants to the Cooperative Health Research in South Tyrol (CHRIS) study, with complete genotype and electrocardiographic data included in the second CHRIS data release on participants recruited between 2011 and 2014. Briefly, the CHRIS study is a population-based cohort study being conducted since 2011 in the Val Venosta/Vinschgau district (South Tyrol, Italy) (Pattaro et al. 2015; Noce et al. 2017). Data include socio-demographic, health, and lifestyle information collected through questionnaires-based interviews and quantitative traits assessed through clinical examinations and urine and blood sampling under overnight fasting conditions.

Replication of genetic associations was tested in MICROS and SHIP. The Microisolates in South Tyrol (MICROS) study (Pattaro et al. 2007) was a cross-sectional, population-based study conducted in three Alpine villages of the same Val Venosta/Vinschgau district where also the discovery CHRIS study was conducted. Considered for replication were 636 individuals who did not participate to the CHRIS study, to guarantee sample independence.

The Study of Health in Pomerania (SHIP-TREND) is a longitudinal population-based cohort study in West Pomerania, a region in the northeast of Germany, assessing the prevalence and incidence of common population-relevant diseases and their risk factors. Baseline examinations for SHIP-TREND were carried out between 2008 and 2012, comprising 4,420 participants aged 20 to 81 years. Study design and sampling methods were previously described (Völzke et al. 2022).

Study outcomes and exclusions

Primary outcomes were the duration of the P-wave, PR, QRS and QT intervals, reflecting atrial and ventricular depolarization and repolarization. We obtained data from 10 s ECGs performed using standard 12-lead ECG workstations: PC-ECG-System Custo 200– Customed (CHRIS); Mortara Portrait, Mortara Inc., Milwaukee, USA (MICROS); Personal 120LD, Esaote, Genova, Italy (SHIP-START and SHIP-TREND). In all studies, participants were asked to remain silent and in supine position during the procedure. Participants with history of atrial fibrillation,

myocardial infarction, heart failure, Wolff-Parkinson-White syndrome, assuming class I and III antiarrhythmics and/or digoxin, pacemaker carriers, and pregnant women, were excluded from the analyses as detailed in Online Resource 1 (Table S1). Values of ECG traits outside the range (1st quartile– 3*interquartile range) and (3rd quartile + 3*interquartile range) were further removed. Between-trait pairwise correlations were estimated by the Pearson's correlation coefficient.

Genotyping

CHRIS and MICROS DNA samples were genotyped using the Illumina HumanOmniExpressExome Bead array. Genotyped SNPs were retained if they had call rate > 99%, Hardy Weinberg Equilibrium (HWE) P-value $\geq 3 \times 10^{-8}$, and minor allele frequency ≥ 0.01. Samples with evidence of sex mismatch, duplication and labelled as outliers after principal component analysis were removed. Data were imputed against the 1000 Genome Phase 1 dataset (1000G.Ph1) using ShapeIT2 and Minimac3 (Das et al. 2016), on GRCh37 assembly.

In SHIP-START, DNA samples were genotyped on the Affymetrix Genome-Wide Human SNP Array 6.0. Excluded were samples with call rate < 86% and SNPs with position mapping issues, HWE P-value ≤ 0.0001, call rate ≤ 0.8, or monomorphic. In SHIP-TREND, DNA samples were genotyped on the Illumina Human Omni 2.5 array. Excluded were samples with call rate < 94% and SNPs with position mapping issues, HWE P-value ≤ 0.0001, call rate ≤ 0.9 or monomorphic. Samples were excluded from both SHIP-START and SHIP-TREND in case of duplication or sex mismatch. Both studies imputed their genotypes with IMPUTE v2.2.2 (Howie et al. 2009) against 1000G.Ph1 (interim).

Genetic association analysis in the CHRIS study

In the CHRIS genomic dataset, we selected the regions encompassing linkage disequilibrium (LD) blocks originating inside the desmosomal genes *DSP*, *PKP2*, *DGS2*, *DSC2*, and *JUP*, and extending outside the gene boundaries. LD-blocks were defined based on the D' confidence intervals (Zapata et al. 1997) and identified applying LDExplorer to the 1000G.Ph3 European-ancestry panel (Taliun et al. 2014).

Association between dosage levels and ECG traits was tested using a genome-wide association study-like approach based on EMMAX as implemented in EPACTS v3.2.6 (Kang et al. 2010), adjusting for age and sex, assuming a genetic additive model, and accounting for relatedness, estimated on the genotyped autosomal variants. The statistical significance level was set at 2.6×10^{-4}, corresponding to the ratio between the genome-wide significance level of 5×10^{-8} to the fraction of genome tested (the LD regions around the 5 desmosomal genes covered approximately 3000 megabases; Table 2). Significantly associated variants were re-tested using appropriate linear mixed model fitting through *lmekin* function implemented in the R package 'coxme' v2.2.5: models included fixed effects for age and sex, and random effect for the day of recruitment, to remove potential long-term recruitment effects (Noce et al. 2017). Relatedness was modeled as in EMMAX within the variance-covariance matrix.

We performed two sensitivity analyses: additionally adjusting for RR interval and BMI; and applying the rank-based inverse normal transformation to the ECG traits. Regional association plots were generated with LocusZoom v0.4.8 (Pruim et al. 2010). Full results of EMMAX analyses and scripts are provided in Online Resource 3 (Datasets S1-S12) and Online Resource 4.

Replication testing

Direction-consistent replication was tested, based on the same genetic model, in the MICROS study by fitting linear mixed models adjusted for age, sex, village, and relatedness, using the *lmekin* function as above, and in SHIP-START and SHIP-TREND by fitting a simple linear models adjusted for age and sex. The Bonferroni-corrected significance level for replication was set to 0.017 (0.05 over 3 variants tested for replication).

Functional, molecular, and clinical annotation

Associated SNPs were annotated using the Ensembl Variant Effect Predictor tool available in Ensembl GRCh37 (http://www.ensembl.org/Tools/VEP), the UCSC genome browser (genome.ucsc.edu), and the SCREEN Encode tool (https://screen.encodeproject.org/) (GRCh37). LD of the CHRIS sample was estimated using LocusZoom v0.4.8 (Pruim et al. 2010), using the–vcf option.

We checked whether the associated variants were associated with other traits at the genome-wide significance level of 5×10^{-8}, including diseases, DNA methylation levels, gene expression, and protein levels, interrogating the PhenoScanner v2 (last accessed on 13/02/2024) (Kamat et al. 2019), the Genotype-Tissue Expression GTEx Project database v8 (GTEx Consortium 2020), and the methylation mQTLdb database (Gaunt et al. 2016).

DNA methylation analyses

We accumulated genomic association with DNA methylation sites from the Framingham Heart Study (FHS),

SHIP-TREND, and the Kooperative Gesundheitsforschung in der Region Augsburg (KORA) FF4 study.

All details regarding sample preparation, methylation analyses and data analyses are described in the Online Resource 4. Prior to MR, we performed a fixed-effects meta-analysis of the association between rs2076298 and cg02643433 in the three above mentioned studies using the command *metan* implemented in Stata 18 (details in Online Resource 2, Figure S5).

Mendelian randomization (MR) analyses

We conducted two-sample MR analyses selecting SNPs as instrumental variables (IV) and retrieving summary statistics of association from published GWAS (GTEx Consortium 2020; Gaunt et al. 2016) and from the current analysis in CHRIS. To satisfy the assumption of relevance, we selected genetic variants associated with the exposure at genome-wide significance level ($p < 5 \times 10^{-8}$) with F statistic > 10. To ensure IVs independency, we selected variants with LD $r^2 < 0.01$. LD was estimated using the Ensemble LD Calculator using the 1000G.Ph3 European ancestry panel as reference (https://www.ensembl.org/Homo_sapiens/Tools/LD).

For each exposure, we could identify only one single SNP satisfying the MR assumptions for use as IV. To exclude the presence of pleiotropy, and hence verifying the exclusion restriction assumption, we inspected available biological evidence from the literature. Following effect allele and direction harmonization between exposures and outcomes, MR estimates were computed as the Wald ratio estimate, with the standard error derived via delta method approximation, using the R package 'MendelianRandomization' v0.9.0 (Patel et al. 2023). Because we were interested in dissecting two alternative pathways, significance level was set at 0.05/2 = 0.025. MR scripts and data are provided in Online Resource 4 and Online Resource (Dataset S15).

Statistical colocalization analyses

We performed statistical colocalization analysis (Giambartolomei et al. 2014) of *DSP-AS1* expression in left ventricle with *DSP* expression in the same tissue and with QRS duration (Fig. 3, pathways E, F), using the *coloc* package v 5.1.0 implemented in R. The data used for the analyses described in this manuscript were obtained from the GTEx Portal on 11/15/24. All analyses were conducted within ± 100 kb from rs2076298, which was selected as instrumental variable in the MR analysis.

Functional follow-up

Cell cultures

For the initial analysis of endogenous *DSP* and lncRNA expression, we used human induced pluripotent stem cells (hiPSC), hiPSC-derived cardiomyocytes (iPSC-CMs), commercial adult human primary keratinocytes (HPK), and human embryonic kidney HEK293T cell lines. HPK were cultured in keratinocyte growth medium (Human EpiVita Serum-Free Growth Medium 141-500a, Cell Applications) HEK293T cells were grown as previously described (Obergasteiger et al. 2023). The hiPSCs line available for this study derives from one healthy individual who was previously characterized (De Bortoli et al. 2023; Meraviglia et al. 2021). Briefly, hiPSCs were cultured in feeder-free conditions on 6-well plates coated with Matrigel (Corning), using a ready-to-use, commercially available medium (StemMACS™ iPS-Brew XF; Miltenyi Biotec). The cardiomyogenic differentiation was induced with the PSC Cardiomyocyte Differentiation Kit (Thermo Fisher Scientific). After 22–25 days of cardiomyogenic differentiation, the beating monolayer of cells was dissociated by Multi Tissue Dissociation Kit 3 (Miltenyi Biotec) to obtain a purified iPSC-CMs population, through the depletion of non-CMs cells, by using PSC-Derived Cardiomyocyte Isolation Kit (Miltenyi Biotec). The purified hiPSC-CMs were replated on matrigel coated 24-well plates (150.000-200.000 cells/well) in a basal medium (High Glucose DMEM; Gibco), 2% Hyclone Fetal Bovine Defined (GE Healthcare Life Sciences), 1% non-essential Amino Acids (Gibco), 1% Penicillin/Streptomycin (Gibco) and 0.09% β-mercapto-ethanol (Gibco) for further experiments. After 3–4 days of recovery, the purified hiPSC-CMs were treated with GapmerRs as described below.

GapmeRs design and delivery in hiPSC-CMs

For the lncRNA knockdown, specific locked nucleic acid (LNA) antisense GapmeRs targeting RP3-512B11.3 lncRNA (Transcript Annotation ENST00000561592.1_1) were designed using the Qiagen RNA Silencing tool, available at https://geneglobe.qiagen.com/us/customize/rna-silencing. The tool ranked several GapmeRs at the highest score. Two were selected, named LNA1 and LNA2, and tested in hiPSC-CMs together with the GapmerR negative control A (NC; LG00000002-FFA, Qiagen).

Four different conditions were tested, at GapmeRs concentrations of: (1) 500nM for 5 days; (2) 500nM for 10 days; (3) 1000nM for 5 days; and (4) 1000nM for 10 days. In all

conditions, the delivery of GapmeRs into hiPSC-CMs was performed through an unassisted "naked" uptake, that is, GapmeRs were directly added to cell medium without transfection reagents. This approach, also known as *gymnosis*, is less toxic for the cells and shows a higher efficiency in cells that are difficult to be transfected as hiPSC-CMs (Anderson et al. 2020; Trembinski et al. 2020). To perform *gymnosis*, the *in vivo ready* high-quality grade (HPLC purification with a final step of sodium salt exchange) was required for the GapmeRs production. For conditions 2 and 4, after 5 days of treatment, the culture medium was replaced with fresh medium containing the same concentration of GapmerR.

RNA isolation and ddPCR analysis.

Total RNA was extracted from cultured cells by TRIzol reagent and Direct-zol RNA Kit (Zymo Research). Then, reverse transcription of 50ng RNA was performed using SuperScript VILO cDNA Synthesis Kit (Invitrogen) in a total volume of 20 µl. Droplet Digital PCR (ddPCR) was performed using a QX200 system (Bio-Rad) according to manufacturer's recommendations. The reactions (22 µl total volume) contained 2× ddPCR™ Supermix for Probes (no dUTP) (Bio-Rad), 20× primer/probe assay for each target, except for *DSP* for which it contained 31.5× primer/probe assay, 1 ng of cDNA for *DSP* and 4ng of cDNA for the *DSP-AS1* lncRNA, and water up to the total volume. For the specific detection of the lncRNA *DSP-AS1*, *DSP* and the reference *RPP30* gene, the following primer/probe assays were used: Bio-Rad qhsaLEP0147498 (FAM), Bio-Rad dHsaCPE5047954 (FAM) and Bio-Rad dHsaCPE5038241 (HEX), respectively. The droplets were generated with the QX200™ Droplet Generator (Bio-Rad), mixing 20 µl of the reactions described above and 70 µl of Droplet Generation Oil for Probes (Bio-Rad), loaded in the proper lanes of DG8™ cartridges. Droplets were then transferred to a 96-well PCR semi-skirted plate and the reaction was performed using a GeneAmp™ PCR System 9700 (Applied Biosystems), according to the following program: 95 °C for 10 min, then 45/40 (*DSP*/*DSP-AS1*) cycles of (94 °C for 30 s, 57/60°C (*DSP*/*DSP-AS1*) for 2 min), 98 °C for 10 min and 4 °C for the storage. Amplification signals were read using the QX200™ Droplet Reader (Bio-Rad) and analyzed using the QuantaSoft software (Bio-Rad). All ddPCR details are described following the Minimum Information for Publication of Digital PCR Experiments (dMIQE) guidelines checklist (dMIQE Group 2020) and are available in Online Resource 1 (Table S10).

Desmoplakin protein expression analysis

RIPA lysis buffer, composed of 10 mM Tris-HCl pH 7.4, 150 mM NaCl, 1% Igepal CA630 (NP-40), 1% sodium deoxycholate (NaDoc), 0.1% SDS (Sodium Dodecyl Sulfate), 1% Glycerol, supplemented with protease and phosphatase inhibitors (Complete Tablets, Mini EASYpack, Roche) was used to lysate hiPSC-CMs, after GapmeRs treatment. The protein level was quantified using Pierce™ BCA Protein Assay Kit (Thermo Scientific).

hiPSC-CMs lysates were tested for desmoplakin protein (sc-390975 mouse anti desmoplakin I/II (A-1), Santa Cruz) and total protein (Total Protein Detection Module, Bio-Techne) using a 66–440 kDa Separation Module (Bio-Techne) on the Protein Simple Wes™ system (Bio-Techne). Lysates were diluted with 0.1X Sample Buffer to a final concentration of 0.2 µg/µl, then mixed with 5X Fluorescent Master Mix and heated at 95 °C for 5 min. Mouse anti-desmoplakin antibody was used at 1:25 dilution, total protein biotin labelling reagent reconstitution mix was prepared following the manufacturer's instructions and then loaded with prepared samples and other reagents (ladder, blocking antibody diluent, HRP-conjugated anti mouse secondary antibody (Anti-Mouse Detection Modules, Bio-Techne), total protein streptavidin HRP and the luminol-peroxide mixture) in the assay plate. We used the following specific instrument settings: *total protein size* as assay type, separation run at 475 V for 30 min, incubation time of 30 min for total protein biotin labelling, total protein streptavidin HRP, primary and secondary antibodies. High dynamic range (HDR) function was applied for luminol/peroxide chemiluminescence detection.

Data analysis

Results of these laboratory experiments were visually inspected via paired dot-plots ("pairplot"). Given hiPSC-CMs obtained from the same differentiation were split into two groups, one treated with LNA2 and the other with LNA-CN, distributions of mRNA expression and protein levels were compared across using the Wilcoxon matched-pairs signed rank test to account for the matched conditions. Because prior evidence was either available or could be hypothesized for the direction of the effect, we applied a one-sided test.

Statistical analysis software

When not otherwise specified, statistical analyses of population data were performed using the R software package (www.R-project.org) (R Core Team 2017). Laboratory experiment data were analyzed with GraphPad version 9.3.1.471.

Results

Genetic association analysis

The overall study design and results are presented in Fig. 1. Discovery and replication study participants characteristics are outlined in Table 1. In the CHRIS study, ECG traits were approximately normally distributed, with low-to-null pairwise correlation: the Pearson's correlation coefficient *r* ranged between 0.09 and 0.21, except for the correlation between PR and P-wave ($r = 0.50$; Online Resource 2 Figure S1).

We identified 29 non-overlapping linkage disequilibrium (LD) blocks originating inside and entirely covering the five desmosomal genes *DSP*, *PKP2*, *DSG2*, *DSC2*, and *JUP*, totalling 570.2 Kb (0.57 Mb), encompassing 2742 single nucleotide polymorphisms (SNPs), imputed on the 1000 Genome Phase 1 dataset (median imputation quality score = 0.92; Table 2).

All SNPs were screened for association with the P-wave, PR, QRS, and QT lengths, using EMMAX approximate linear mixed modelling (Kang et al. 2020), accounting for multiple testing. As displayed by the regional association plots (Fig. 2A; Online Resource 2 Figure S2), we identified significant associations of rs2744389 in *DSP* with QRS (P-value $= 3.7 \times 10^{-5}$), two nearly independent variants rs115171396 and rs72835665 in *JUP* (LD $r^2 = 0.017$) with P-wave length (P-values $= 2.4 \times 10^{-5}$ and 6.7×10^{-5}), and rs13412, a missense variant in *P3H4* falling within the *JUP* LD region, with QT (P-value $= 1.8 \times 10^{-5}$; Online Resource 1 Table S2). All results were robust to inverse normal transformation of the traits and to adjustment for body mass index (BMI) and the RR interval, except for rs13412, whose association with QT which was not significant anymore after BMI and RR adjustment (Online Resource 1 Table S2). We thus excluded rs13412 from further analyses. Significant results were refined using appropriate linear mixed modelling in R (Table 3): we observed an effect of −1.10 ms on QRS per copy of the rs2744389 effect allele, which was replicated in the MICROS study (one-sided P-value = 0.010; Table 3), with a very similar effect size of −1.47 ms QRS length per copy of the effect allele. This association did not replicate in the SHIP-START and SHIP-TREND cohorts. The associations of rs115171396 and rs72835665 in *JUP* with P-wave were not replicated in any study (Table 3). Analysis of QRS conditional on rs2744389 didn't identify any additional independently associated variant.

Functional annotation and phenotypic interrogation

rs2744389 is located in the first intron of *DSP*, immediately downstream the promoter and within a strong enhancer element characterized by H3K4Me1 and H3K27Ac marks, colocalizing with a DNAse I hypersensitivity element; the enhancer is active in the heart right atrium and left ventricle (Fig. 2B). Additionally, rs2744389 is in linkage disequilibrium with variants found in patients with ACM and cardiocutaneous syndromes (Online Resource 1 Table S3). The genomic region selected for association testing included two validated pseudogenes (*RPS26P29* ribosomal protein S26 pseudogene 29, and *IDH1P1* isocitrate dehydrogenase (NADP+) 1 pseudogene 1) and a long non-coding antisense RNA overlapping the DSP promoter, *DSP-AS1* (Fig. 2B), with rs2744389 falling in the first exon of *DSP-AS1*. The function of the processed pseudogenes is currently unknown, and their expression was nearly undetectable in any tissue of the GTEx v8 dataset (GTEx Consortium 2020). *DSP-AS1* has an expression pattern very similar to *DSP*, but ~10-fold lower (Online Resource 2 Figure S3), and its function was unknown.

We interrogated the GWAS catalog and PhenoScanner (Kamat et al. 2019) databases, searching for additional, genome-wide significant associations of rs2744389 with any complex trait, identifying a significant association with pulse rate (P-value $= 1.5 \times 10^{-13}$) in the UK Biobank (Bycroft et al. 2018).

UCSC genome browser interrogation identified SNPs within the analyzed region that were in strong LD with rs2744389 (LD D'>0.80) and significantly associated with ECG traits (Online Resource 2 Figure S4): rs7771320 (D'=0.81, $r^2 = 0.30$) with the QRS 12-lead-voltage duration products (12-leadsum) (van der Harst et al. 2016); rs112019128 (D'=0.89, $r^2 = 0.43$) with the PR interval (Ntalla et al. 2020); rs72825038 (D'=0.94, $r^2 = 0.46$) with PR interval (Ntalla et al. 2020) and ECG morphology (amplitude at temporal datapoints, Verweij et al. 2020); and rs72825047 with spatial QRS-T angle (Young et al. 2023). The rs2744389 itself showed some evidence of association with ECG morphology (Verweij et al. 2020) (P-value $= 2 \times 10^{-6}$).

In GTEx, rs2744389 C allele was associated with higher *DSP-AS1* expression, which was maximal in the adrenal gland, but not with *DSP* expression (Online Resource 1 Table S4). No genome-wide significant DSP eQTL was annotated in GTEx v8. rs2744389 was also associated with methylation of cg02643433, located in the CpG island 201 in the first intron of *DSP*: this association was direction-consistent across multiple datasets (Online Resource 1

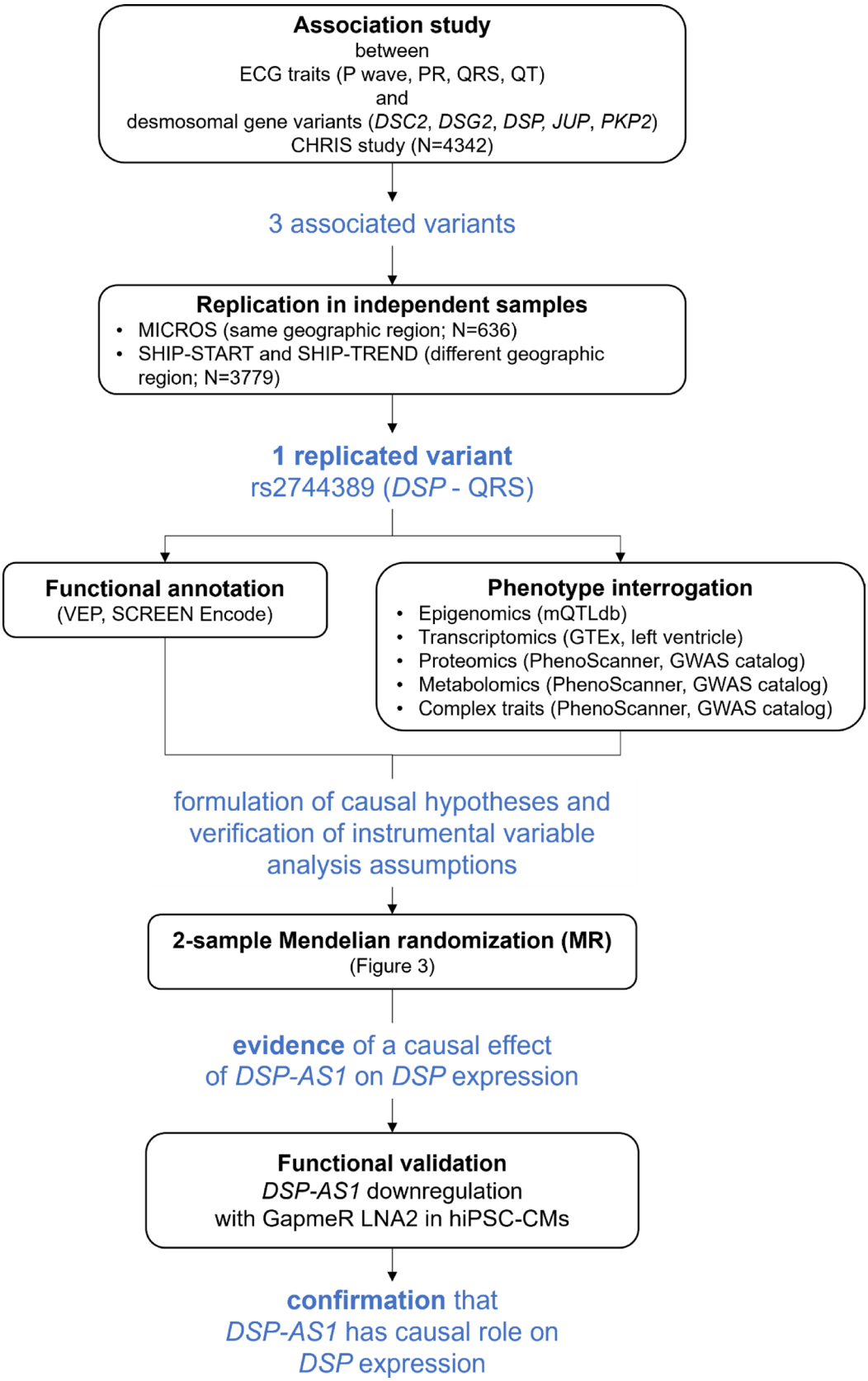

Fig. 1 Analysis flowchart and main results

Table 1 Discovery and replication sample description

	CHRIS (*N*=4342)	MICROS (*N*=636)	SHIP-START (*N*=2957)	SHIP-TREND (*N*=822)
Age (years)	46(16)	44(17)	48(16)	49(14)
Women (N, %)	2426(56)	326(51)	1521(51)	458(56)
BMI (kg/m^2)	25.6(4.6)	25.3(4.7)	27.1(4.8)	27.0(4.5)
RR (ms)	1013.8(155.5)	909.0(160.4)	NA	NA
P-wave (ms)	105.9(12.2)	101.1(5.4)	110.2(11.3)	113.6(11.8)
PR (ms)	158.1(24.2)	NA	NA	NA
QRS (ms)	95.7(9.3)	95.5(9.4)	97.0(10.7)	94.7(11.0)
QT (ms)	413.9(28.8)	NA	NA	NA

ECG statistics are calculated after trait-specific clinical exclusions (Online Resource 1 Table S1). Mean and standard deviations (in brackets) describe quantitative variables

ms millisecond, *NA* not available

Table S4). We didn't observe evidence of associations with protein levels or metabolites.

Mendelian randomization (MR) and colocalization analyses

Motivated by this overall evidence, rather than focusing on the functional characterization of the intronic rs2744389, which looks more a classical "tag" variant, we hypothesized that cg02643433 and *DSP-AS1* could regulate *DSP* expression, which could in turn causally affect QRS duration. We therefore tested the concatenation of causal effects depicted in Fig. 3 using the two-sample MR technique. We first tested the causal effect of cg02643433 methylation on the RNA levels of *DSP-AS1* (Fig. 3, pathway A) and *DSP* (Fig. 3, pathway B), and on QRS duration (Fig. 3, pathway C). To this end, we extracted genetic variants associated with cg02643433 methylation from mQTLdb (Gaunt et al. 2016), choosing methylation levels from blood of the middle age group, and from GTEx v8 heart left ventricle, which was the most relevant tissue available for the current investigation.

Next, we tested the causal effect of *DSP-AS1* expression on *DSP* expression (Fig. 3, pathway D), on QRS duration (Fig. 3, pathway E) and reverse causation on cg02643433 methylation (Fig. 3, pathway F). The latter was tested in consideration of biological evidence showing that antisense RNA can modify DNA methylation (Mattick et al. 2023). We extracted genetic variants associated with *DSP-AS1* expression from the GTEx v8 left ventricle dataset and from the Framingham Heart Study (FHS) (Huan at al. 2019), the SHIP-TREND and KORA FF4 studies in whole blood for testing reverse causation (Fig. 3, pathway F).

Because we could not find any SNP genome-wide significantly associated with *DSP* mRNA level in the left ventricle, and no desmoplakin protein GWAS was available, we couldn't test further questions such as for instance whether the desmoplakin protein levels affect QRS duration.

Studies used to identify the IV summary statistics are described in Online Resource 1 Table S5. As strong IVs (P-value$<5\times10^{-8}$; F statistic>10), we identified 26 and 119 SNPs associated with cg02643433 methylation (Online Resource 1 Table S6) and *DSP-AS1* expression in left ventricle (Online Resource 1 Table S7), respectively. LD pruning ($r^2>0.01$; Online Resource 3 Datasets S13, S14) left a single IV per exposure: rs7767989 for cg02643433 and rs2076298 for *DSP-AS1* (Fig. 2B; Table 4). Scientific literature examination showed that selected IVs were not associated with other traits than the selected exposures. Variants in LD with them were associated with cardiovascular and ECG-related phenotypes or pulmonary phenotypes. The rs2076295 was associated with levels of the receptor for advanced glycation product RAGE, a cell surface pattern receptor recognizing multiple ligands, mostly expressed in the lung and involved in inflammation. Overall, available evidence suggests that vertical pleiotropy could exist (cardiovascular traits) but horizontal pleiotropy violating MR assumptions is unlikely (Online Resource 1 Table S8).

cg02643433 methylation was causally associated with increased QRS duration (P-value=0.002); *DSP-AS1* expression was causally associated with decreased QRS duration (P-value=0.015; Table 4) and decreased *DSP* expression in the heart left ventricle (P-value$=6.33\times10^{-5}$). This latter

Table 2 Selected gene regions

Gene name (abbreviation)	Location (GRCh37) chr: bp	Selected regions based on LD blocks chr: bp	Region size (Kb)	Number of LD blocks	Number of SNPs identified	Rsq (median, IQR)
Desmocollin 2 (*DSC2*)	18:28,645,940−28,682,378	18:28,624,553−28,721,059	96.5	3	272	0.95(0.64–0.99)
Desmoglein 2 (*DGS2*)	18:29,078,006–29,128,971	18:29,075,273−29,136,399	61.1	2	377	0.99(0.81-1.00)
Desmoplakin (*DSP*)	6:7,541,808-7,586,950	6:7,501,701-7,590,326	88.6	9	526	0.93(0.69–0.98)
Junction Plakoglobin (*JUP*)	17:39,775,692−39,943,183	17:39,775,870−39,967,442	191.6	10	861	0.85(0.61–0.95)
Plakophilin 2 (*PKP2*)	12:32,943,679−33,049,774	12:32,938,452−33,070,666	132.2	5	706	0.97(0.80-1.00)
Total			570.0	29	2742	0.92(0.70–0.99)

chr chromosome, *bp* base-pairs, *LD* Linkage Disequilibrium, *Rsq* imputation quality score, *IQR* interquartile range

finding supports an antisense-mediated mechanism of gene expression regulation, where an antisense RNA (*DSP-AS1*) downregulates its target (*DSP*). Confounding by LD was ruled out by evidence of colocalization between *DSP-AS1* and *DSP* expression in left ventricle (PP_{H4}=0.91; Online Resource 1 Table S9). Colocalization between *DSP-AS1* expression and QRS could not be proven (PP_{H4}=0.09), likely because the QRS association peak was not pronounced (PP_{H1}=0.73).

DSP-AS1 and *DSP* mRNA expression in different cell types

To validate the causal effect of *DSP-AS1* on *DSP* expression (Fig. 3 pathway E), we conducted a series of in vitro experiments. We first tested whether *DSP-AS1* and *DSP* mRNA were expressed in keratinocytes, human induced pluripotent stem cells (hiPSCs), hiPSC-derived cardiomyocytes (hiPSC-CMs), and HEK cells, using digital droplet PCR (ddPCR). Both transcripts were expressed in all tested cells, at various degrees, with keratinocytes and HEK cells expressing the highest and lowest *DSP* levels, respectively. *DSP-AS1* was less expressed than *DSP* in all cell lines, showing the highest expression in HEK and the lowest in hiPSC-CMs (Online Resource 2 Figure S6). Given our initial interest in desmosomal genes as genetic causes of ACM, we proceeded with the functional follow-up by downregulating *DSP-AS1* in hiPSC-CMs, the gold standard in cell cardiac research.

DSP-AS1 downregulation in hiPSC-CMs

We treated hiPSC-CMs with two GapmeRs, LNA1 and LNA2, plus a negative control GapmerR, LNA_NC, testing different conditions. All GapmeRs were delivered to cells by gymnosis. The LNA2 induced *DSP-AS1* downregulation under all tested conditions. LNA1 treatment showed no effect, like LNA_NC, for which treated cells didn't show differences compared to non-treated cells (NT) (Online Resource 2 Figure S7). We repeated hiPSC-CMs treatment with LNA2 at 1000nM for 10 days, confirming a ~ 2.5-fold downregulation of *DSP-AS1* compared to LNA_NC-treated cells (Fig. 4A).

DSP-AS1 downregulation leads to an increased Desmoplakin mRNA and protein levels in hiPSC-CMs

We then tested whether *DSP-AS1* downregulation could affect *DSP* mRNA expression using ddPCR, observing evidence of a significant ~ 1.5-fold increase in *DSP* mRNA level following *DSP-AS1* downregulation by LNA2 (Fig. 4B). We finally tested whether desmoplakin protein levels were also affected by *DSP-AS1* downregulation using the Protein

Table 3 Genetic association results

				CHRIS			MICROS				SHIP-START + SHIP-TREND			
Trait	SNP, gene	Chr: bp*	Alleles†	N	EAF	Beta(SE)	P-value	N	EAF	Beta(SE)	P-value‡	N	EAF	Beta(SE)	P-value‡
P-wave	rs115171396, *JUP*	17:39910519	C/T	4338	0.02	4.87(1.08)	6.6×10^{-6}	636	0.02	−0.19(3.12)	0.525	3779	0.01	1.59(1.45)	0.136
P-wave	rs72835665, *JUP*	17:39922558	G/A	4338	0.51	−1.10(0.27)	4.5×10^{-5}	636	0.56	0.18(0.87)	0.585	3779	0.53	−0.06(0.29)	0.416
QRS	rs2744389, *DSP*	6:7543123	A/C	4259	0.18	−1.10(0.24)	3.5×10^{-6}	626	0.18	−1.47(0.64)	0.010	3661	0.16	0.21(0.32)	0.748

chr chromosome, *bp* base-pairs, *EAF* effect allele frequency, *Beta* effect per copy of the effect allele in ms, *SE* Standard Error of Beta

*Build GRCh37 †Reference/Effect allele ‡One-sided

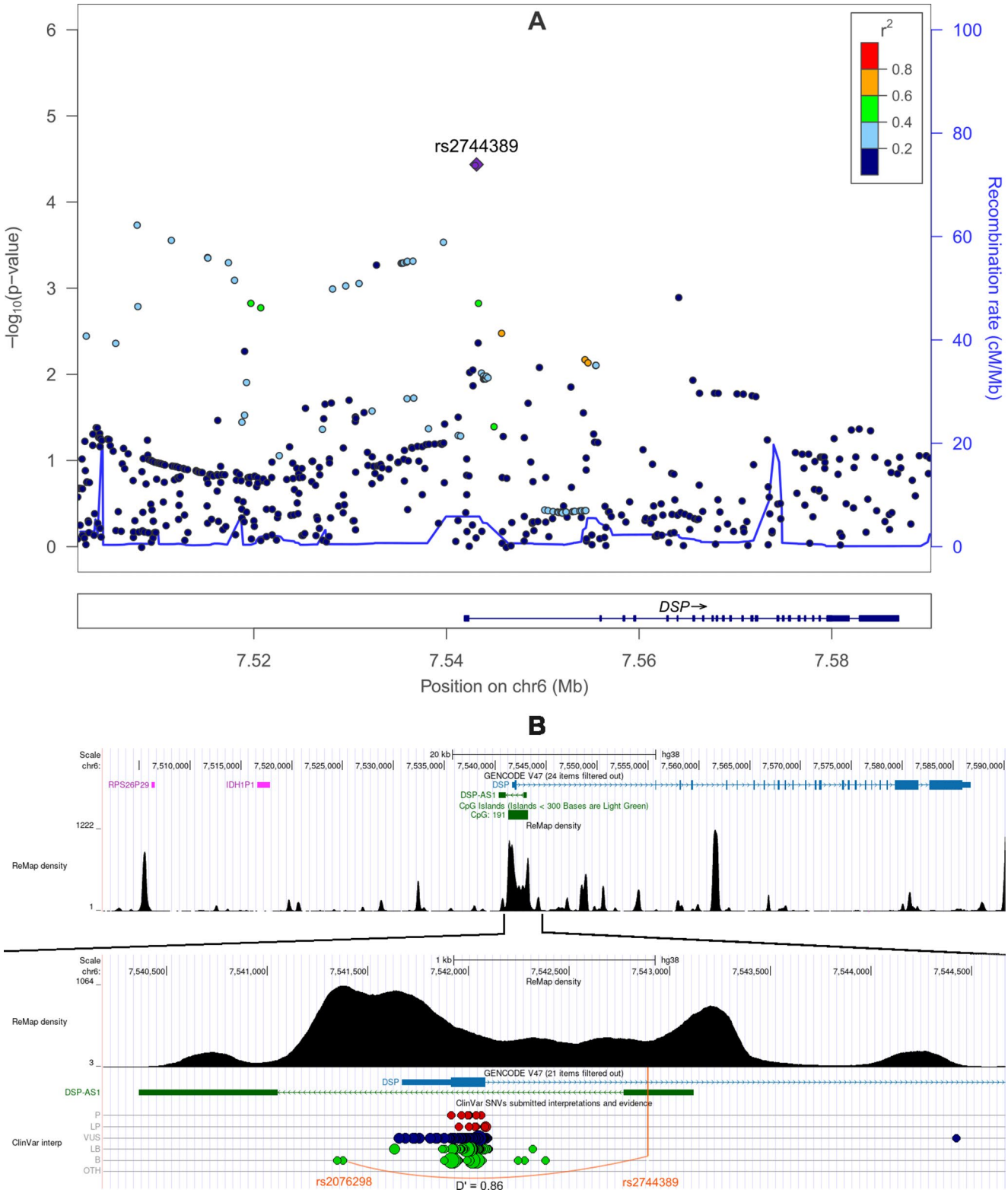

Fig. 2 Regional association plot showing association of the *DSP* genomic context with QRS length. **A** -log10(*P*-value) of the SNP-QRS association (y-axis) against SNP genomic position (GRCh37; x-axis) at *DSP*. The purple diamond indicates the most associated SNP (position 7,543,123); its LD with the other SNPs is based on the r^2 estimated on the CHRIS sample. **B** Annotated genomic context, including validated pseudogenes, ReMap track showing multiple regulatory elements condensed, and ClinVar track. Orange vertical line: rs2744389 location. LD with rs2076298, selected IV for MR, is also highlighted. Figure source: UCSC genome browser

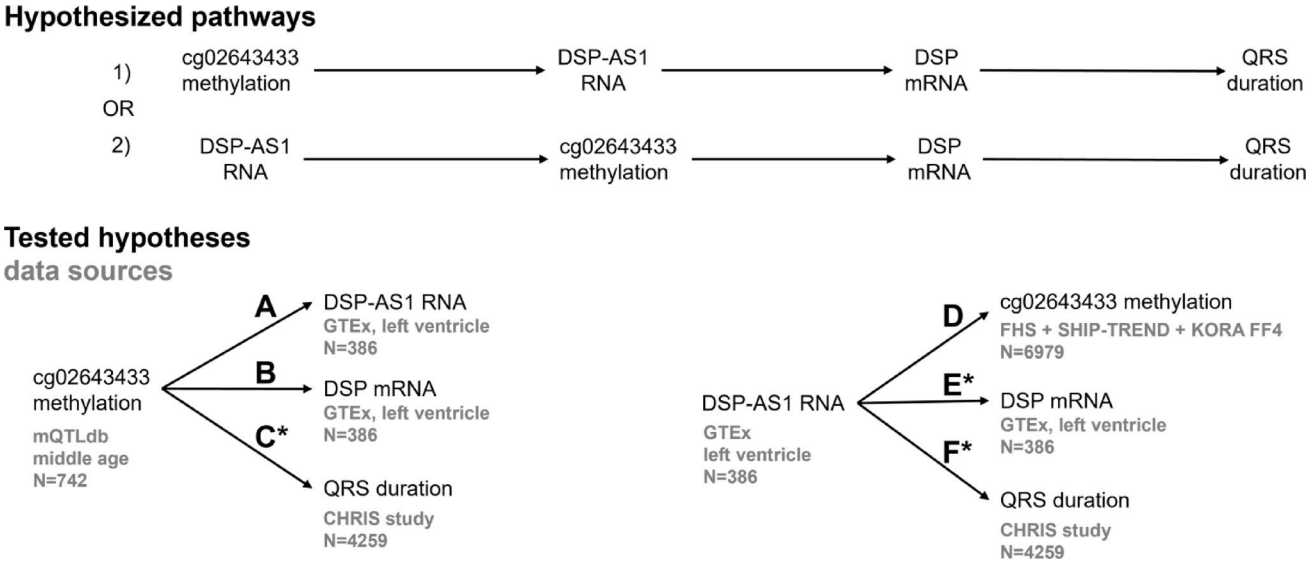

Fig. 3 Mendelian randomization analysis scheme. Upper panel: overview of the two hypothesized biological pathways underlying *DSP* regulation, possibly contributing to QRS duration. Lower panel: decomposition of the pathways by individual analysis with indication of the instrumental variable and data sources. Causal effect of cg02643433 methylation on *DSP-AS1* mRNA level (**A**), *DSP* mRNA level (**B**), and QRS duration (**C**); causal effect of *DSP-AS1* RNA level on cg02643433 methylation (**D**), *DSP* mRNA (**E**, experimentally validated), and QRS duration (**F**). The causal effect of *DSP* mRNA on desmoplakin protein levels was not tested due to the lack of proteome-wide association studies including desmoplakin. *denotes significant MR results (Table 4)

Simple Wes™ system, observing a protein upregulation of ~1.5-fold in LNA2-treated cells (Fig. 4C).

Discussion

By combining genomic and clinical data from population-based studies with in vitro functional experiments, we demonstrated that downregulating *DSP-AS1* lncRNA expression causes an increase of *DSP* mRNA and protein level. Additionally, *DSP-AS1* resulted being causally associated with QRS duration.

LncRNAs have been recently recognized as key regulators of multiple cellular functions, from the arrangement of chromatin architecture to the regulation of RNA transcription and post-transcriptional modifications, protein synthesis and localization (Mattick et al. 2023). However, they remain poorly characterized by scarce functional studies. In cardiovascular disease, dysregulated lncRNAs contribute to various mechanisms, including endothelial dysfunction and myocardial remodeling and some of them serve as biomarkers for disease diagnosis and prognosis (Fang et al. 2020).

Previous studies identified three *DSP*-targeting lncRNAs in non-cardiac tissues and cell lines: *MIR4435-2HG* (Wang et al. 2019) and *UPLA1* (*GJD3-AS1*) (Han et al. 2020), respectively promoting gastric cancer and lung adenocarcinoma progression, that target desmoplakin, leading to Wnt/β-catenin signaling pathway activation; and *LYPLAL1-AS1* (Yang et al. 2021), which directly binds desmoplakin, possibly targeting it to proteasome degradation, resulting in Wnt/β-catenin pathway signaling downregulation and human adipose-derived mesenchymal stem cells adipogenic differentiation. In summary, lncRNA-mediated *DSP* downregulation leads to both Wnt/β-catenin pathway activation (cancer cells) and inhibition (adipogenic differentiation), a contrasting behaviour that has been previously reported in ACM (Lorenzon et al. 2017).

Our findings add a novel, *cis*-acting mechanism of antisense-mediated *DSP* gene regulation, differently from the above mentioned *trans*-acting lncRNAs. Unlike the latter, which play structural roles or regulate proteins and other RNAs through direct interactions and require high expression levels, *cis*-acting lncRNAs can effectively target a single gene with few molecules (Statello et al. 2021). *DSP* and *DSP-AS1* are transcribed bidirectionally, with divergent transcription, overlapping with a head-to-head configuration (Werner et al. 2024). Hypermethylation upstream and immediately downstream of the *DSP* transcriptional start site overlapping *DSP-AS1* was detected in lung cancer cell lines, leading to decreased *DSP* levels and Wnt/β-catenin

Table 4 Mendelian randomization analysis results

Exposure (X)							Outcome (Y)				Mendelian randomization	
Exposure	IV	EA	EAF	Beta(SE)	P-value	F	Outcome	EAF	Beta(SE)	P-value	Beta(SE)	P-value
cg02643433	rs7767989	C	0.37	−0.49(0.04)	2.83×10^{-29}	151.15	DSP-AS1	0.37	−0.02(0.03)	0.554	0.04(0.06)	0.505
							DSP mRNA	0.37	−0.01(0.02)	0.584	0.02(0.04)	0.617
							QRS	0.36	−0.55(0.18)	2.40×10^{-3}	1.12(0.37)	0.002
DSP-AS1	rs2076298	C	0.46	0.28(0.03)	5.55×10^{-22}	108.17	DSP mRNA	0.46	−0.08(0.02)	1.03×10^{-4}	−0.29(0.07)	6.33×10^{-5}
							QRS	0.48	−0.46(0.19)	0.016	−1.67(0.69)	0.015
							cg02643433	0.47	−0.003(0.002)	0.082	−0.01(0.01)	0.134

Results of the analyses presented in Fig. 3. Exposure summary statistics obtained from: mQTLdb database, middle age $N = 742$ (cg02643433); GTEx, left ventricle $N = 386$ (*DSP-AS1*). Outcome summary statistics obtained from: GTEx left ventricle $N = 386$ (*DSP-AS1; DSP*); CHRIS study $N = 4259$ (QRS); FHS $N = 4170$, SHIP-TREND $N = 964$, KORA FF4 $N = 1928$ (cg02643433)

EA Effect Allele, *EAF* Effect Allele Frequency, *Beta* effect per copy of the effect allele, *SE* standard error of Beta

pathway activation as previously reported (Yang et al. 2012). Differential methylation of the *DSP* conserved promoter was also observed in human and mouse lung epithelial cells seeded on matrigel-coated soft or stiff polyacrylamide gels, showing opposite effects (Qu et al. 2018). We speculate that *DSP-AS1* may be involved in the regulation of *DSP* expression controlling chromatin architecture acting on DNA methylation, a hypothesis that we have tested but could not be confirmed within our MR framework (*P*-value = 0.134). However, as our MR analyses were based on summary statistics available on methylation data from blood only, and DNA methylation is tissue specific, additional experiments are warranted on cardiac-specific methylation data.

Clarifying *DSP-AS1* mechanism of action is relevant, also in light that ACM caused by *DSP* pathogenic variants is currently regarded as a distinct clinical entity called Desmoplakin cardiomyopathy. Patients exhibit acute myocardial injury episodes, inflammation and extensive left ventricular involvement even at early disease stages, with an aggressive arrhythmic course, that was recently characterized in depth (Smith et al. 2020; Gasperetti et al. 2025). A review of the ARVD/C Genetic Variants Database (https://arvc.molgeniscloud.org/menu/main/home) revealed seven variants in exon 1 (p.Gln51X; p.Val30Met; p.Tyr42=; p.Gly35=; p.Gly46Asp; p.Leu26=; p.Thr49Ser) and one variant in 5'UTR (c.1dupA). It is therefore crucial to ascertain the impact of variants in the *DSP-AS1* regions that overlap with *DSP*, to establish a more precise genotype-phenotype relation. Loss of functional *DSP* was rescued in a zebrafish model, through genetic and pharmacological manipulations, leading to Wnt/β-catenin activation and consequent beneficial effects (Giuliodori et al. 2018). Findings disagree with a more recent work showing that suppression rather than activation of the Wnt/β-catenin pathway is beneficial in desmoplakin cardiomyopathy (Olcum et al. 2023). Altogether, *DSP* appears as an actionable target that could be manipulated by acting on *DSP-AS1*, resulting in a possible strategy for increasing desmoplakin protein level in *DSP* haploinsufficient ACM patients. Because *DSP* is also involved in dilated cardiomyopathy, cardio cutaneous disorders, cancer and lung diseases, targeting *DSP-AS1* could also have additional applications.

All causal and downstream analyses started by observing the QRS-rs2744389 association in CHRIS, which was replicated in MICROS, a small study conducted in the same Alpine area (Pattaro et al. 2007). MICROS participants who joined the CHRIS study were removed from the analysis, guaranteeing separate samples. The similarity of the allelic

effects on QRS between the two studies is remarkable. The association did not replicate in SHIP-START and SHIP-TREND, conducted in Northern Germany.

The replication of the association of rs2744389 in MICROS but not in SHIP could lie in the characteristics of the locus, perhaps sensitive to environmental exposures, hence in a possible gene-environment interaction (Kraft et al. 2009). CHRIS and MICROS participants live in a mountainous region at moderate-to-high altitude as opposed to SHIP participants live at the sea level. ECG is known to change in response to chronic altitude exposure (Parodi et al. 2023). However, this hypothesis remains to be proven. Additionally, despite all participants to the four studies were of European descent, there might be differences in the genetic architecture in terms of population-specific LD patterns (Sirugo et al. 2019), which was observed to affect genomic associations also within Europe (Hamet et al. 2017). As also the CHARGE consortium GWAS of QRS (Young et al. 2022) did not identify genome-wide significant associations at this locus, it is likely that we are in the presence of heterogeneous LD structure at the locus or environmental interaction. Nevertheless, genome-wide significant associations with QRS-related traits were observed for SNPs in LD with rs2744389: rs7771320 (D'=0.81) associated with the QRS complex 12-lead sum (van der Harst et al. 2016) and rs72825038 (D'=0.94) associated with QRS morphology (Verweij et al. 2020). In LD were also rs112019128 and rs72825038, previously associated with PR interval by the CHARGE consortium (Ntalla et al. 2020) but not significant in CHRIS. These findings corroborate the relevance of *DSP* and its promoter region in association with ECG regulations in general population individuals, not necessarily affected by cardiac pathologies.

Our work has both strengths and limitations. We depicted a pipeline for a candidate gene approach and downstream analyses, applying MR to prioritize potential causal targets for subsequent functional follow-up. The main strength is the in vitro validation of the causal effect of *DSP-AS1* on *DSP* gene observed with MR. The validation is particularly relevant because it overcomes a major limitation of our two-sample MR analysis between *DSP-AS1* and *DSP* expression, where the IV summary statistics for both exposure and outcome were extracted from the same GTEx heart left ventricle sample, resulting in full overlap. Sample overlap may bias MR estimates (Burgess et al. 2016), even if a recent investigation showed reassuring results that two-sample MR methods can be applied to a one-sample framework without major risks of bias (Minelli et al. 2021). Another major limitation was the impossibility to test all possible causal links in the depicted pathways, due to the absence of appropriate IVs for some variables. Additionally, methylation QTL were derived from blood and not from cardiac tissues. We were also unable to perform a multivariate MR, due to presence of a single IV for the exposures of interest. Finally, while being beyond the scope of this investigation, the exact molecular mechanism linking rs2744389 alleles to *DSP-AS1* expression in a causal manner remains unknown. The most likely explanation is that the association reflects LD of rs2744389 with *DSP-AS1* functional variants.

Conclusions

In conclusion, genomics analyses of desmosomal genes in association with ECG traits in a general population sample, identified a variant associated with QRS length located in the promoter region of *DSP*, at the *DSP-AS1* lncRNA. Downstream causal analyses provided evidence of a potential novel antisense-mediated mechanisms controlling *DSP* expression in *cis*. This evidence was finally corroborated by in vitro GapmeR analysis, proving that *DSP-AS1* can regulate *DSP* expression both at mRNA and protein levels. Additional experimental investigations are warranted to clarify the *DSP-AS1* mechanisms of action. These should include a fine analysis of the *DSP-AS1/DSP* promoter sequence to determine the impact of variants on *DSP* expression and on the three-dimensional structure, stability and function of *DSP-AS1*. While *DSP-AS1* represents a potential target for treatment of diseases caused by *DSP* mutations, such as ACM, dilated cardiomyopathy, cardiocutaneous diseases (e.g. Carvajal syndrome) and some cancer conditions, further investigations are warranted to test the identified GapmeR on hiPSC-CMs carrying a desmoplakin mutation causing a protein deficit. Such models could ideally envision the use of advanced engineered heart tissue platforms, efficiently simulating physiological conditions (Bliley et al. 2021).

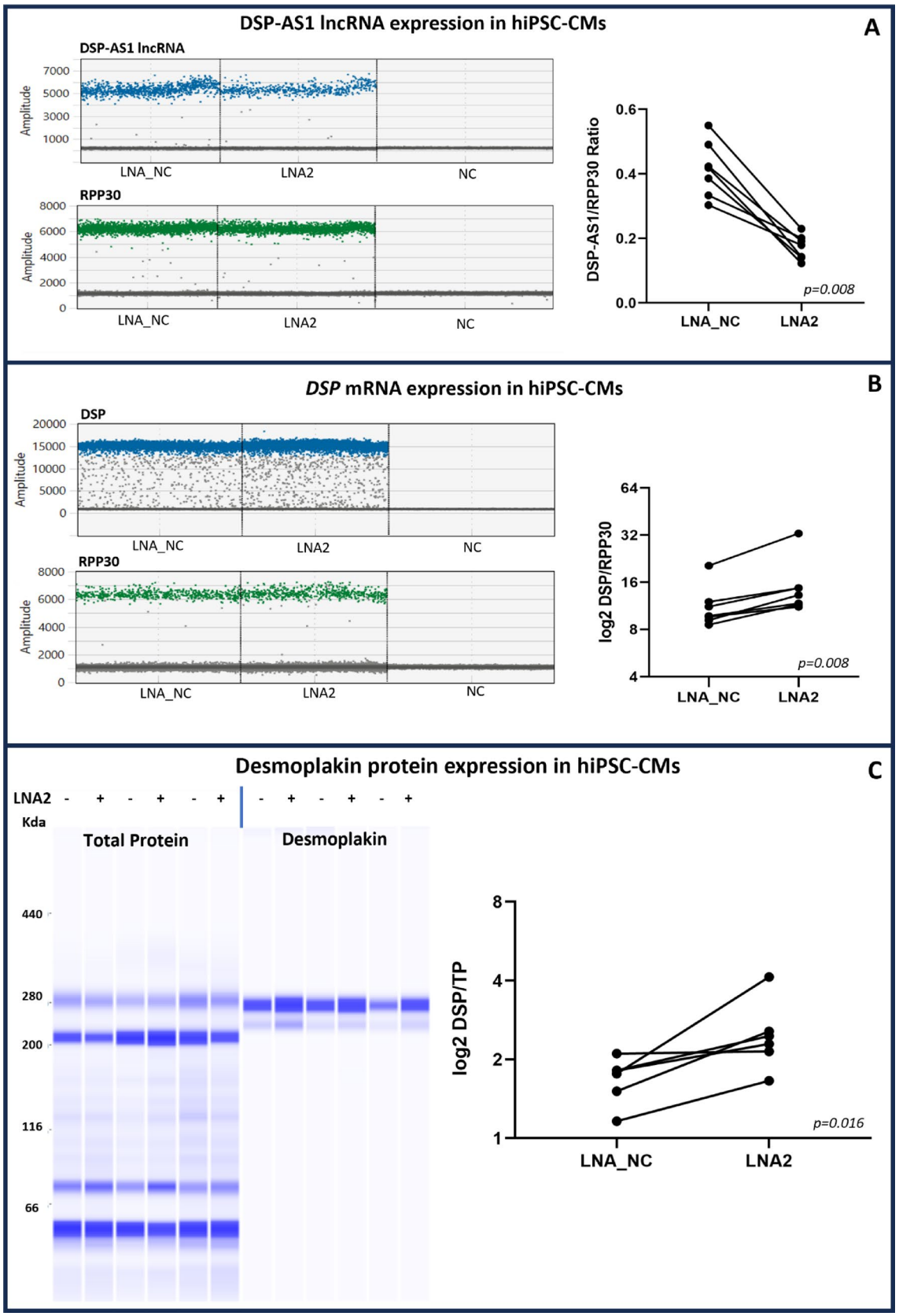
DSP-AS1 lncRNA expression in hiPSC-CMs
A
DSP-AS1 lncRNA
Amplitude
7000
5000
3000
1000
LNA_NC
LNA2
NC
RPP30
8000
6000
4000
2000
0
DSP-AS1/RPP30 Ratio
0.6
0.4
0.2
0.0
p=0.008
DSP mRNA expression in hiPSC-CMs
B
DSP
20000
15000
10000
5000
log2 DSP/RPP30
64
32
16
8
4
p=0.008
Desmoplakin protein expression in hiPSC-CMs
C
LNA2
Kda
Total Protein
Desmoplakin
440
280
200
116
66
log2 DSP/TP
8
4
2
1
p=0.016

Fig. 4 In vitro validation of the causal effect of *DSP-AS1* on *DSP* mRNA and protein levels. Effect of treatment of hiPSC-CMs with LNA control (LNA-NC) and LNA2 GapmerR at 1000nM for 10 days (LNA2). Data were available on 7 independent cardiomyogenic differentiations. Each dot in the pairplot represents an independent differentiation; lines in the pairplot connect the same differentiation to highlight the change in the measured outcomes after treatment with LNA2. **A** Relative expression of *DSP-AS1* after LNA2 treatment (*P*-value=0.008). **B** Relative expression of DSP mRNA after LNA2 treatment (*P*-value=0.008). NC: negative control; RPP30: reference gene; amplitude indicates the fluorescence intensity of each probe; in blue, the FAM channel for *DSP-AS1* and *DSP;* in green, the HEX channel for RPP30. **C** Relative abundance of desmoplakin protein after LNA2 treatment (*P*-value=0.016). TP: Total protein. All data were analysed using a one-sided Wilcoxon matched-pairs signed rank test. Raw data are provided in Online Resource 1 Tables S13, S14 and S15

Supplementary Information The online version contains supplementary material available at https://doi.org/10.1007/s00439-025-02761-x.

Acknowledgements We thank all CHRIS, MICROS, SHIP, KORA, and FHS participants. The CHRIS study thanks the Healthcare System of the Autonomous Province of Bolzano/Bozen - South Tyrol (https://www.eurac.edu/chrisack). Bioresource Impact Factor Code: BRIF6107. The MICROS study was supported by the Ministry of Health of the Autonomous Province of Bolzano/Bozen - South Tyrol and the South Tyrolean Sparkasse Foundation. We thank all collaborators of both Eurac Research and the Healthcare System of the Autonomous Province of Bolzano/Bozen - South Tyrol who made the CHRIS and MICROS studies possible. The SHIP authors are grateful to Paul S. DeVries for his support with the EWAS pipeline. We thank all participants for their long-term commitment to the KORA study, the staff for data collection and research data management and the members of the KORA Study Group (https://www.helmholtz-munich.de/en/epi/cohort/kora) who are responsible for the design and conduct of the study. We thank Emilio Cusanelli for his precious suggestions on lncRNA's science. The authors thank the Department of Innovation, Research University and Museums of the Autonomous Province of Bozen/Bolzano for covering the Open Access publication costs.

Author contributions Conceptualization: LF, MDB, AR, CP; data curation: LF, MDB, FDGM, CF, MG; formal data analysis: LF, MDB, TD, TH, AT; funding acquisition: MDB, PPP, AR, CP; experimental investigation: MDB, LSF, CV, DAR, BMM; supervision: MDB, UV, JW, MD, DL, MW, AR, CP; original draft preparation: LF, MDB, CP. All authors read and approved the final manuscript.

Funding CHRIS study was funded by the Autonomous Province of Bolzano/Bozen - South Tyrol - Department of Innovation, Research, University and Museums and supported by the European Regional Development Fund (FESR1157). MICROS was supported by the Ministry of Health of the Autonomous Province of Bolzano and the South Tyrolean Sparkasse Foundation. This study was supported by the Department of Innovation, Research and University of the Autonomous Province of Bolzano (Italy) and by the Joint Project Alto Adige-SNSF (Italy-Switzerland) to MDB. SHIP is part of the Community Medicine Research net of the University of Greifswald, Germany, which is funded by the Federal Ministry of Education and Research (grants no. 01ZZ9603, 01ZZ0103, and 01ZZ0403), the Ministry of Cultural Affairs as well as the Social Ministry of the Federal State of Mecklenburg-West Pomerania, and the network 'Greifswald Approach to Individualized Medicine (GANI_MED)' funded by the Federal Ministry of Education and Research (grant 03IS2061A). Genome-wide data have been supported by the Federal Ministry of Education and Research (grant no. 03ZIK012) and a joint grant from Siemens Healthineers, Erlangen, Germany and the Federal State of Mecklenburg-West Pomerania. DNA methylation data have been supported by the DZHK (grants 81X3400104, 81X2400157). The KORA study was initiated and financed by the Helmholtz Zentrum München– German Research Center for Environmental Health, which is funded by the German Federal Ministry of Education and Research (BMBF) and by the State of Bavaria. Data collection in the KORA study is done in cooperation with the University Hospital of Augsburg.

Data availability The CHRIS analyzed data and samples can be requested for clearly defined research activities via the CHRIS Portal (https://chrisportal.eurac.edu/). SHIP data can be requested via https://transfer.ship-med.uni-greifswald.de. All the experimental raw data supporting the conclusions of this article are available in Online Resource 1, Tables S11-S15.

Declarations

Competing interests CP has received consultant fees from Quotient Therapeutics. All other authors declared no conflicts of interest.

Ethics approval and consent to participate CHRIS study was approved by the Ethics Committee of the Healthcare System of the Autonomous Province of Bolzano/Bozen, South Tyrol (approval number 21-2011). MICROS study was approved by the Provincial Ethics Committee of Bolzano/Bozen - South Tyrol (23.5 Dr.MVH/31.05.07.14/19644) with an update approved by the Ethics Committee of the Healthcare System of the Autonomous Province of Bolzano/Bozen - South Tyrol (18/09/2013). The research involving human stem cell lines was approved by the Ethics Committee of the Province of Bolzano (approval number 1/2014). SHIP-START and SHIP-TREND were approved by the Ethics Committee at the University Medicine Greifswald (approval number BB 39/08). The studies conform to the Declaration of Helsinki, and with national and institutional legal and ethical requirements. All participants included in the analysis gave oral and written informed consent.

References

Anderson BR, Jensen ML, Hagedorn PH, Little SC, Olson RE, Ammar R et al (2020) Allele-Selective knockdown of MYH7 using antisense oligonucleotides. Mol Ther Nucleic Acids 19:1290–1298. https://doi.org/10.1016/j.omtn.2020.01.012

Austin KM, Trembley MA, Chandler SF, Sanders SP, Saffitz JE, Abrams DJ et al (2019) Molecular mechanisms of arrhythmogenic

cardiomyopathy. Nat Rev Cardiol 16(9):519–537. https://doi.org/10.1038/s41569-019-0200-7

Blair DR, Lyttle CS, Mortensen JM, Bearden CF, Jensen AB, Khiabanian H et al (2013) A nondegenerate code of deleterious variants in Mendelian loci contributes to complex disease risk. Cell 155(1):70–80. https://doi.org/10.1016/j.cell.2013.08.030

Bliley JM, Vermeer MCSC, Duffy RM, Batalov I, Kramer D, Tashman JW et al (2021) Dynamic loading of human engineered heart tissue enhances contractile function and drives a desmosome-linked disease phenotype. Sci Transl Med 13(603):eabd1817. https://doi.org/10.1126/scitranslmed.abd1817

Burgess S, Davies NM, Thompson SG (2016) Bias due to participant overlap in two-sample Mendelian randomization. Genet Epidemiol 40(7):597–608. https://doi.org/10.1002/gepi.21998

Bycroft C, Freeman C, Petkova D, Band G, Elliott LT, Sharp K et al (2018) The UK biobank resource with deep phenotyping and genomic data. Nature 562(7726):203–209. https://doi.org/10.1038/s41586-018-0579-z

Chen SN, Gurha P, Lombardi R, Ruggiero A, Willerson JT, Marian AJ (2014) The Hippo pathway is activated and is a causal mechanism for adipogenesis in arrhythmogenic cardiomyopathy. Circ Res 114(3):454–468. https://doi.org/10.1161/CIRCRESAHA.114.302810

Das S, Forer L, Schönherr S, Sidore C, Locke AE, Kwong A et al (2016) Next-generation genotype imputation service and methods. Nat Genet 48(10):1284–1287. https://doi.org/10.1038/ng.3656

De Bortoli M, Meraviglia V, Mackova K, Frommelt LS, König E, Rainer J et al (2023) Modeling incomplete penetrance in arrhythmogenic cardiomyopathy by human induced pluripotent stem cell derived cardiomyocytes. Comput Struct Biotechnol J 21:1759–1773. https://doi.org/10.1016/j.csbj.2023.02.029

dMIQE Group, Huggett JF, The Digital MIQE (2020) Guidelines update: minimum information for publication of quantitative digital PCR experiments for 2020. Clin Chem 66(8):1012–1029. https://doi.org/10.1093/clinchem/hvaa125

Elliott PM, Anastasakis A, Asimaki A, Basso C, Bauce B, Brooke MA et al (2019) Definition and treatment of arrhythmogenic cardiomyopathy: an updated expert panel report. Eur J Heart Fail 21(8):955–964. https://doi.org/10.1002/ejhf.1534

Fang Y, Xu Y, Wang R, Hu L, Guo D, Xue F et al (2020) Recent advances on the roles of LncRNAs in cardiovascular disease. J Cell Mol Med 24(21):12246–12257. https://doi.org/10.1111/jcmm.15880

Garcia-Gras E, Lombardi R, Giocondo MJ, Willerson JT, Schneider MD, Khoury DS et al (2006) Suppression of canonical Wnt/beta-catenin signaling by nuclear Plakoglobin recapitulates phenotype of arrhythmogenic right ventricular cardiomyopathy. J Clin Invest 116(7):2012–2021. https://doi.org/10.1172/JCI27751

Gasperetti A, Carrick RT, Protonotarios A, Murray B, Laredo M, van der Schaaf I et al (2025) Clinical features and outcomes in carriers of pathogenic Desmoplakin variants. Eur Heart J 46(4):362–376. https://doi.org/10.1093/eurheartj/ehae571

Gaunt TR, Shihab HA, Hemani G, Min JL, Woodward G, Lyttleton O et al (2016) Systematic identification of genetic influences on methylation across the human life course. Genome Biol 17:61. https://doi.org/10.1186/s13059-016-0926-z

Giambartolomei C, Vukcevic D, Schadt EE, Franke L, Hingorani AD, Wallace C et al (2014) Bayesian test for colocalisation between pairs of genetic association studies using summary statistics. PLoS Genet 10(5):e1004383. https://doi.org/10.1371/journal.pgen.1004383

Giuliodori A, Beffagna G, Marchetto G, Fornetto C, Vanzi F, Toppo S et al (2018) Loss of cardiac Wnt/β-catenin signalling in desmoplakin-deficient AC8 zebrafish models is rescuable by genetic and Pharmacological intervention. Cardiovasc Res 114(8):1082–1097. https://doi.org/10.1093/cvr/cvy057

GTEx Consortium (2020) The GTEx consortium atlas of genetic regulatory effects across human tissues. Science 369(6509):1318–1330. https://doi.org/10.1126/science.aaz1776

Hamet P, Haloui M, Harvey F, Marois-Blanchet FC, Sylvestre MP, Tahir MR et al (2017) PROX1 gene CC genotype as a major determinant of early onset of type 2 diabetes in Slavic study participants from action in diabetes and vascular disease: preterax and diamicron MR controlled evaluation study. J Hypertens 35(Suppl 1Suppl 1):S24–32. https://doi.org/10.1097/HJH.0000000000001241

Han X, Jiang H, Qi J, Li J, Yang J, Tian Y et al (2020) Novel LncRNA UPLA1 mediates tumorigenesis and prognosis in lung adenocarcinoma. Cell Death Dis 11(11):999. https://doi.org/10.1038/s41419-020-03198-y

Howie BN, Donnelly P, Marchini J (2009) A flexible and accurate genotype imputation method for the next generation of genome-wide association studies. PLoS Genet 5(6):e1000529. https://doi.org/10.1371/journal.pgen.1000529

Huan T, Joehanes R, Song C, Peng F, Guo Y, Mendelson M et al (2019) Genome-wide identification of DNA methylation QTLs in whole blood highlights pathways for cardiovascular disease. Nat Commun 10(1):4267. https://doi.org/10.1038/s41467-019-12228-z

James CA, Jongbloed JDH, Hershberger RE, Morales A, Judge DP, Syrris P et al (2021) International evidence based reappraisal of genes associated with arrhythmogenic right ventricular cardiomyopathy using the clinical genome resource framework. Circ Genom Precis Med 14(3):e003273. https://doi.org/10.1161/CIRCGEN.120.003273

Kamat MA, Blackshaw JA, Young R, Surendran P, Burgess S, Danesh J et al (2019) PhenoScanner V2: an expanded tool for searching human genotype-phenotype associations. Bioinformatics 35(22):4851–4853. https://doi.org/10.1093/bioinformatics/btz469

Kang HM, Sul JH, Service SK, Zaitlen NA, Kong SY, Freimer NB et al (2010) Variance component model to account for sample structure in genome-wide association studies. Nat Genet 42(4):348–354. https://doi.org/10.1038/ng.548

Kraft P, Zeggini E, Ioannidis JPA (2009) Replication in genome-wide association studies. Stat Sci 24(4):561–573

Lahtinen AM, Lehtonen E, Marjamaa A, Kaartinen M, Heliö T, Porthan K et al (2011) Population-prevalent desmosomal mutations predisposing to arrhythmogenic right ventricular cardiomyopathy. Heart Rhythm 8(8):1214–1221. https://doi.org/10.1016/j.hrthm.2011.03.015

Lorenzon A, Calore M, Poloni G, De Windt LJ, Braghetta P, Rampazzo A (2017) Wnt/β-catenin pathway in arrhythmogenic cardiomyopathy. Oncotarget 8(36):60640–60655. https://doi.org/10.18632/oncotarget.17457

Mattick JS, Amaral PP, Carninci P, Carpenter S, Chang HY, Chen LL et al (2023) Long non-coding rnas: definitions, functions, challenges and recommendations. Nat Rev Mol Cell Biol 24(6):430–447. https://doi.org/10.1038/s41580-022-00566-8

Meraviglia V, Cattelan G, De Bortoli M, Motta BM, Volpato C, Frommelt LS et al (2021) Generation and characterization of three human induced pluripotent stem cell lines (EURACi007-A, EURACi008-A, EURACi009-A) from three different individuals of the same family with arrhythmogenic cardiomyopathy (ACM) carrying the plakophillin2 p.N346Lfs*12 mutation. Stem Cell Res 55:102466. https://doi.org/10.1016/j.scr.2021.102466

Minelli C, Del Greco MF, van der Plaat DA, Bowden J, Sheehan NA, Thompson J (2021) The use of two-sample methods for Mendelian randomization analyses on single large datasets. Int J Epidemiol 50(5):1651–1659. https://doi.org/10.1093/ije/dyab084

Noce D, Gögele M, Schwienbacher C, Caprioli G, De Grandi A, Foco L et al (2017) Sequential recruitment of study participants May

inflate genetic heritability estimates. Hum Genet 136(6):743–757. https://doi.org/10.1007/s00439-017-1785-8

Ntalla I, Weng LC, Cartwright JH, Hall AW, Sveinbjornsson G, Tucker NR et al (2020) Multi-ancestry GWAS of the electrocardiographic PR interval identifies 202 loci underlying cardiac conduction. Nat Commun 11(1):2542. https://doi.org/10.1038/s41467-020-15706-x

Obergasteiger J, Castonguay AM, Pizzi S, Magnabosco S, Frapporti G, Lobbestael E et al (2023) The small GTPase Rit2 modulates LRRK2 kinase activity, is required for lysosomal function and protects against alpha-synuclein neuropathology. NPJ Parkinsons Dis 9(1):44. https://doi.org/10.1038/s41531-023-00484-2

Olcum M, Fan S, Rouhi L, Cheedipudi S, Cathcart B, Jeong HH et al (2023) Genetic inactivation of β-catenin is salubrious, whereas its activation is deleterious in Desmoplakin cardiomyopathy. Cardiovasc Res 119(17):2712–2728. https://doi.org/10.1093/cvr/cvad137

Parodi JB, Ramchandani R, Zhou Z, Chango DX, Acunzo R, Liblik K et al (2023) A systematic review of electrocardiographic changes in healthy high-altitude populations. Trends Cardiovasc Med 33(5):309–315. https://doi.org/10.1016/j.tcm.2022.01.013

Patel A, Ye T, Xue H, Lin Z, Xu S, Woolf B et al (2023) MendelianRandomization v0.9.0: updates to an R package for performing Mendelian randomization analyses using summarized data. Wellcome Open Res 8:449. https://doi.org/10.12688/wellcomeopenres.19995.1

Pattaro C, Marroni F, Riegler A, Mascalzoni D, Pichler I, Volpato CB et al (2007) The genetic study of three population microisolates in South Tyrol (MICROS): study design and epidemiological perspectives. BMC Med Genet 8:29. https://doi.org/10.1186/1471-2350-8-29

Pattaro C, Gögele M, Mascalzoni D, Melotti R, Schwienbacher C, De Grandi A et al (2015) The cooperative health research in South Tyrol (CHRIS) study: rationale, objectives, and preliminary results. J Transl Med 13:348. https://doi.org/10.1186/s12967-015-0704-9

Pruim RJ, Welch RP, Sanna S, Teslovich TM, Chines PS, Gliedt TP et al (2010) LocusZoom: regional visualization of genome-wide association scan results. Bioinformatics 26(18):2336–2337. https://doi.org/10.1093/bioinformatics/btq419

Qu J, Zhu L, Zhou Z, Chen P, Liu S, Locy ML et al (2018) Reversing mechanoinductive DSP expression by CRISPR/dCas9-mediated epigenome editing. Am J Respir Crit Care Med 198(5):599–609. https://doi.org/10.1164/rccm.201711-2242OC

R Core Team (2017) R: A Language and environment for statistical computing. R Foundation for Statistical Computing, Vienna, Austria

Schinner C, Xu L, Franz H, Zimmermann A, Wanuske MT, Rathod M et al (2022) Defective desmosomal adhesion causes arrhythmogenic cardiomyopathy by involving an Integrin-αVβ6/TGF-β signaling cascade. Circulation 146(21):1610–1626. https://doi.org/10.1161/CIRCULATIONAHA.121.057329

Sen-Chowdhry S, Syrris P, McKenna WJ (2005) Genetics of right ventricular cardiomyopathy. J Cardiovasc Electrophysiol 16(8):927–935. https://doi.org/10.1111/j.1540-8167.2005.40842.x

Sharma A, Bosman LP, Tichnell C, Nanavati J, Murray B, Nonyane BAS et al (2022) Arrhythmogenic right ventricular cardiomyopathy prevalence and arrhythmic outcomes in At-Risk family members: A systematic review and Meta-Analysis. Circ Genom Precis Med 15(3):e003530. https://doi.org/10.1161/CIRCGEN.121.003530

Sirugo G, Williams SM, Tishkoff SA (2019) The missing diversity in human genetic studies. Cell 177(1):26–31. https://doi.org/10.1016/j.cell.2019.02.048

Smith ED, Lakdawala NK, Papoutsidakis N, Aubert G, Mazzanti A, McCanta AC et al (2020) Desmoplakin cardiomyopathy, a fibrotic and inflammatory form of cardiomyopathy distinct from typical dilated or arrhythmogenic right ventricular cardiomyopathy. Circulation 141(23):1872–1884. https://doi.org/10.1161/CIRCULATIONAHA.119.044934

Statello L, Guo CJ, Chen LL, Huarte M (2021) Gene regulation by long non-coding RNAs and its biological functions. Nat Rev Mol Cell Biol 22(2):96–118

Taliun D, Gamper J, Pattaro C (2014) Efficient haplotype block recognition of very long and dense genetic sequences. BMC Bioinformatics 15:10. https://doi.org/10.1186/1471-2105-15-10

Towbin JA, McKenna WJ, Abrams DJ, Ackerman MJ, Calkins H, Darrieux FCC et al (2019) 2019 HRS expert consensus statement on evaluation, risk stratification, and management of arrhythmogenic cardiomyopathy. Heart Rhythm 16(11):e301–e372. https://doi.org/10.1016/j.hrthm.2019.05.007

Trembinski DJ, Bink DI, Theodorou K, Sommer J, Fischer A, van Bergen A et al (2020) Aging-regulated anti-apoptotic long noncoding RNA Sarrah augments recovery from acute myocardial infarction. Nat Commun 11(1):2039. https://doi.org/10.1038/s41467-020-15995-2

van der Harst P, van Setten J, Verweij N, Vogler G, Franke L, Maurano MT et al (2016) 52 genetic loci influencing myocardial mass. J Am Coll Cardiol 68(13):1435–1448. https://doi.org/10.1016/j.jacc.2016.07.729

Verweij N, Benjamins JW, Morley MP, van de Vegte YJ, Teumer A, Trenkwalder T et al (2020) The genetic makeup of the electrocardiogram. Cell Syst 11(3):229–238e5. https://doi.org/10.1016/j.cels.2020.08.005

Völzke H, Schössow J, Schmidt CO, Jürgens C, Richter A, Werner A et al (2022) Cohort profile update: the study of health in Pomerania (SHIP). Int J Epidemiol 51(6):e372–e383. https://doi.org/10.1093/ije/dyac034

Wang H, Wu M, Lu Y, He K, Cai X, Yu X et al (2019) LncRNA MIR4435-2HG targets Desmoplakin and promotes growth and metastasis of gastric cancer by activating Wnt/β-catenin signaling. Aging 11(17):6657–6673. https://doi.org/10.18632/aging.102164

Werner A, Kanhere A, Wahlestedt C, Mattick JS (2024) Natural antisense transcripts as versatile regulators of gene expression. Nat Rev Genet. https://doi.org/10.1038/s41576-024-00723-z

Yang L, Chen Y, Cui T, Knösel T, Zhang Q, Albring KF et al (2012) Desmoplakin acts as a tumor suppressor by Inhibition of the Wnt/β-catenin signaling pathway in human lung cancer. Carcinogenesis 33(10):1863–1870. https://doi.org/10.1093/carcin/bgs226

Yang Y, Fan J, Xu H, Fan L, Deng L, Li J et al Long noncoding RNA LYPLAL1-AS1 regulates adipogenic differentiation of human mesenchymal stem cells by targeting Desmoplakin and inhibiting the Wnt/β-catenin pathway. Cell Death Discov 2021 15;7(1):105. https://doi.org/10.1038/s41420-021-00500-5

Young WJ, Lahrouchi N, Isaacs A, Duong T, Foco L, Ahmed F et al (2022) Genetic analyses of the electrocardiographic QT interval and its components identify additional loci and pathways. Nat Commun 13(1):5144. https://doi.org/10.1038/s41467-022-32821-z

Young WJ, Haessler J, Benjamins JW, Repetto L, Yao J, Isaacs A et al (2023) Genetic architecture of Spatial electrical biomarkers for cardiac arrhythmia and relationship with cardiovascular disease. Nat Commun 14(1):1411. https://doi.org/10.1038/s41467-023-36997-w

Zapata C, Alvarez G, Carollo C (1997) Approximate variance of the standardized measure of gametic disequilibrium D'. Am J Hum Genet 61(3):771–774. https://doi.org/10.1016/S0002-9297(07)64342-0

Authors and Affiliations

Luisa Foco[1] · Marzia De Bortoli[1] · Fabiola Del Greco M[1] · Laura S. Frommelt[1,2,3] · Chiara Volani[1,4] · Diana A. Riekschnitz[1] · Benedetta M. Motta[1] · Christian Fuchsberger[1] · Thomas Delerue[5] · Uwe Völker[6,7] · Tianxiao Huan[8,9] · Martin Gögele[1] · Juliane Winkelmann[10] · Marcus Dörr[7,11] · Daniel Levy[8,9] · Melanie Waldenberger[5,12] · Alexander Teumer[7,13] · Peter P. Pramstaller[1] · Alessandra Rossini[1] · Cristian Pattaro[1]

✉ Luisa Foco
luisa.foco@eurac.edu

✉ Cristian Pattaro
cristian.pattaro@eurac.edu

1 Eurac Research, Institute for Biomedicine, Via Volta 21, Bolzano 39100, Italy

2 Department of Life Sciences, University of Trieste, Trieste, Italy

3 Cardiovascular Biology Laboratory, International Centre for Genetic Engineering and Biotechnology (ICGEB), Trieste, Italy

4 The Cell Physiology MiLab, Department of Biosciences, Università degli Studi di Milano, Milano, Italy

5 Research Unit Molecular Epidemiology, Institute of Epidemiology, Helmholtz Munich, 85764 Neuherberg, Germany

6 Interfaculty Institute for Genetics and Functional Genomics, University Medicine Greifswald, Greifswald, Germany

7 DZHK (German Center for Cardiovascular Research), partner site Greifswald, Greifswald, Germany

8 Framingham Heart Study, Framingham, MA, USA

9 The Population Studies Branch, National Heart, Lung, and Blood Institute of the National Institutes of Health, Bethesda, MD, USA

10 Institute of Neurogenomics, Helmholtz Munich, Helmholtz Munich, 85764 Neuherberg, Germany

11 Department SHIP/Clinical-Epidemiological Research, Institute for Community Medicine, University Medicine Greifswald, Greifswald, Germany

12 German Centre for Cardiovascular Research (DZHK), Partner Site Munich Heart Alliance, 81377 Munich, Germany

13 Department of Psychiatry and Psychotherapy, University Medicine Greifswald, Greifswald, Germany